ENCIT 2018

ABCM Associação Brasileira de Engenharia e Ciências Mecânicas

17th Brazilian Congress of Thermal Sciences and Engineering
November 25th-28th, 2018, Águas de Lindóia, SP, Brazil

ENCIT-2018-0300
COMPUTATIONAL FLUID DYNAMICS (CFD) BASED APPROACHES FOR MODELING AIRCRAFT TURBOFANS

Rene Aguilar, Cesar Celis
Mechanical Engineering Section
Pontificia Universidad Católica del Perú
Av. Universitaria 1801, San Miguel, Lima 32, Lima, Perú
h.aguilar@pucp.pe
ccelis@pucp.edu.pe

Marcio Pontes
marciolopespontes@gmail.com

Abstract. *Computational fluid dynamics (CFD) is one of the most important tools in analysis and design of axial turbo machinery as aircraft turbofans or axial compressors. Accordingly, this work presents a review of the state-of-the-art of the main CFD based techniques used for modeling aircraft turbofans. These modeling approaches include the full annulus unsteady Reynolds average Navier Stokes (URANS) simulations, the actuator disc approach, the body force modeling, the frozen rotor model and the mixing planes model. More specifically, comparative analyses of the advantages and limitations of the referred methodologies are initially presented. From the available numerical approaches, the one based on mixing planes is selected for further exploration. The rationale behind the selection of this modeling technique for carrying out turbofan-related simulations in this work is properly highlighted. Finally, numerical simulations of a GE-90 like turbofan engine are carried out using a mixing planes based model. The results obtained from the simulations are discussed in terms of mass, momentum and energy conservation along the turbofan bypass duct. The relative good agreement between the numerical results obtained here and those available in the literature emphasizes the suitability of the modeling approach utilized in this work.*
Keywords: *Aircraft turbofans, computational fluid dynamics, modeling approaches, mixing planes.*

1. INTRODUCTION

Civil aircraft transportation has experienced a continuous increase in contrast with other modes of transportation (Lee et al.,2001). Consequently, according to the International Air Transport Association (IATA), the number of passengers is expected to grow up from 3.3 billion in 2014 to 7 billion in 2034 (IATA, 2015). In addition, Boeing has estimated an increase in aircraft demand of 4.9% for the 2014-2035 period (Boeing, 2012). This results in a direct impact on the actual infrastructure, current aircrafts and the environment (Kellari et al., 2017). On the other hand, it is estimated that aircraft engine fuel efficiency will improve at an average rate of 1.4% per annum to 2040 (1.76% per annum from 2020 to 2030)(International Civil Aviation Organization, 2013). As stated by the International Civil Aviation Organization (ICAO), the main impacts of the aviation trends are the aircraft noise and the gaseous emissions that affect the local air quality and the global climate change (International Civil Aviation Organization, 2013). To address these issues the aircraft manufacturing and airline industries, the scientific community, and governmental bodies have invested large amounts of resources on research programs aiming to improve aircraft performance (Lee et al., 2001).

An aircraft turbofan is a jet engine where one part of the flow passes through a duct to generate thrust, the called bypass-flow, and the other part goes through the compressor, combustor and turbine (core flow) (Kerrebrock, 1992). Turbofan engines are crucial components in modern civil aircrafts. According to *Calvert and Ginder* (1999), the bypass flow accounts for about three quarters of the total engine thrust and it has a significative influence on noise, fuel emissions and weight. Past research works show that the Specific Fuel Consumption (SFC) and noise can be reduced by increasing the by-pass ratio ($BRP = \frac{\dot{m}_{bypass}}{\dot{m}_{core}}$) and reducing the fan pressure ratio (FPR) (Goulos et al., 2018)(Godard et al., 2017)(Cumpsty, 2010). This is why several research works focus for instance on the development of geared low-speed fans (MacIsaac & Langton, 2011), the design of short inlets for low FPR (Peters, 2014) and the impact of bypass nozzles on the engine aerodynamic performance (Goulos et al., 2018). The engine thrust is a function of its bypass ratio and overall pressure ratio, which depend of the engine operating conditions and dimensions. As a result, a high by pass ratio is related to a high both thrust and propulsive efficiency. The increase in the engine mass flow rate has aerodynamic effects on the flow structure over the bypass flow and the exhaust nozzle. Consequently small variations in the bypass duct geometry can lead to decrease the total engine performance (Abdol-Hamid et al. , 1993). Therefore, a better design of the engine bypass duct needs to account for these effects (Goulos et al., 2018). Several techniques have been used for

the design of high bypass ratio turbofans. Broadly speaking these techniques includes experiments and CFD based calculations.

Computational fluid dynamics (CFD) has becoming an essential tool for aerodynamic design of axial turbo-machinery and its components. Modern CFD codes support the numerical modelling of rotating parts like the turbofan rotor. Since the flow structure in the engine bypass flow depends on the distortion produced by rotating parts, the effects of the fan rotor geometry on the flow characteristics need to be accounted for. The main goal of this paper is to examine the flow structure behavior in the bypass region (downstream the fan) using a mixing planes based approach accounting for the fan blade effects. This constitutes the first stage of an ongoing work seeking to analyze ways of improving aircraft turbofan performance. These ways include for instance modifications in the bypass duct geometry (Pontes , 2015) . For this purpose a GE90 like turbofan engine is numerically simulated using CFD where the fan blades are preliminary designed using a first principles-based approach relying on the radial equilibrium theory (Dixon & Hall, 2013).

Accordingly, this work is organized as follows. The second section presents a brief literature review of the main CFD based approaches used for turbofan numerical modeling, including their capabilities and main limitations. Section 3 describes in turn the mathematical model utilized here for modeling the aircraft turbofan engine. The numerical approach, including the engine operating conditions, geometry and meshing details, as well as the boundary conditions used, are described in Section 4. Section 5 presents the main results of the numerical simulations carried out here. Finally, the conclusions drawn from these results are summarized in Section 6.

2. AIRCRAFT TURBOFAN NUMERICAL MODELING APPROACHES

Over the years a large effort has been devoted to the development of computational techniques capable of effectively simulating turbo machinery flows. The flow in a turbo machinery stage is inherently unsteady. This complex flow that can change the stagnation pressure and temperature in a fluid domain has a oscillatory behavior influencing the upstream flow (Greitzer et al., 2004). Adamszyc (2000) argues that the smalls eddy scales present in those flows are due to turbulence and the large scales are linked to the shaft rotational speed. Research work focused on the flow structure through a turbofan stage (Maunus et al. , 2012) suggests that the wakes produced by the fan rotor become more diffuse due to convection in the downstream and spanwise directions.

The main CFD models used for simulating the turbo machinery rotor effects on the flow behavior include the body force modelling, the actuator disc approach, the full annulus unsteady Reynolds Average Navier Stokes (RANS) model and the mixing planes approach. From these techniques, the most utilized one is the mixing planes based model. Indeed, the full annulus unsteady RANS (URANS) modeling is the one that demands the highest computational cost. It consists of simulating, using a RANS formulation, the whole turbofan annulus at unsteady conditions. This is thus one of the most accurate methods to simulate the flow distortion patterns induced by the rotor (Jerez Fidalgo et al., 2012). A number of studies (Jerez Fidalgo et al. ,2012)(Schnell et al. , 2016)(Peters, 2014) have shown the capabilities of this modelling technique to account for fan intake interactions and distorted flows induced by the fan rotor. Other unsteady methods are beyond the scope of this paper but the interested reader may refer to Biesinger et al. (2010).

In the actuator disk model in turn, the meshed fan is replaced by an axial flow sector through which stagnation pressure, enthalpy rise and flow deviation are added (Godard et al., 2017). Notice that the 2D actuator disk does not capture well the swirl effects and usually requires stagnation pressure and temperature tables across the rotor (Peters, 2014). Other works dealing with this particular modelling approach include those by Trancossi & Madonia (2012) and Kim et al. (1999).

In the body force modeling method, the blade rows are replaced with a body force field to capture the interactions between fan and air at a lower computational cost compared to URANS simulations (Thollet et al., 2015). The physical blade effects on the flow domain are due to pressure and viscous forces (Peters, 2014). Notice that the body force field simulates the effect of the discrete blades producing the same stagnation pressure rise and flow turning as the URANS model (Peters, 2014). In this particular model, firstly proposed by Marble (1964), the derived body forces produce a change in swirl and entropy in the rotor flow domain. Besides, the mesh size is drastically reduced due the absence of the fan blade geometries. However, it does not capture well the stage (rotor/stator) interactions (Godard et al., 2017).

The mixing planes method is a steady state approach for modeling turbo machinery stages. In this modeling technique, data from adjacent zones (rotating and stationary domains) are passed as boundary conditions that are spatially averaged or mixed at the mixing plane interface (an interface between rotor and stator). In this method, which was firstly proposed by Denton (1992), the resulting solutions are able to provide reasonable approximations of the time averaged flow field (ANSYS, 2018). Gunaraj et al (2014) verified this modeling approach in the past through a comparison between two fan stage designs. The main outcomes from the referred study indicate that the results obtained from the numerical simulations, in terms of fan stage performance and stalling throttle condition, present a reasonable agreement with engine test ones. Due to its relatively low computational cost, this modeling approach allows carrying out quickly several CFD based engine simulations. Nevertheless, some numerical errors and jumps in the flow field are introduced due the mixing process. A detailed review of the main advantages and limitations of the mixing planes approach for modeling turbomachinery flows be found in Denton (2016) and (Montomoli et al., 2015).

From the four methodologies for turbofan modeling described in this section, the most accurate one is the URANS approach. However, it has the highest computational cost. The body force modeling (BFM) and the actuator disk approach address the inlet and outlet fan distortion interactions, but they need additional data for their modeling such as previous RANS simulations or empirical correlations. Moreover, the referred methods (BFM and Actuator disk) do not have the capability to account for fan rotor stator interactions. The mixing planes approach address the modeling of rotor stator interactions and provides a suitable boundary conditions for the up and downstream frames of reference (fan domain). In addition, this method accounts for the effects of upstream and downstream geometries and has a relatively computational cost due the average process that enables the steady state treatment. Accordingly, this last modeling technique is used in this work.

3. MATHEMATICAL MODELING

A GE90 like turbofan engine has been numerically simulated for the analysis of the flow structure in the engine bypass region. The flow domain solved features two frames of reference, a stationary frame and a rotating are fixed to the rotating parts. The steady state three-dimensional Navier Stokes equations constitutes the governing equations for the stationary frame (Greitzer et al., 2004). Furthermore, for the rotating frame additional terms are added to these equations due the effects of the coriolis and centrifugal accelerations (Greitzer et al., 2004). For the moving frame of reference, the fluid is modeled as at steady state with some limitations (Fluent, 2011). In addition, the ideal gas law is used for accounting for the density changes. The governing equations for the non-inertial rotating frame are given by (Fluent, 2011),

$$\frac{\partial p}{\partial t} + \nabla \cdot \rho\overrightarrow{v_r} = 0 \,, \tag{1}$$

$$\frac{\partial}{\partial t}(\rho\overrightarrow{v_r}) + \nabla \cdot (\rho\overrightarrow{v_r}\overrightarrow{v_r}) + \rho(\vec{\omega} \times \vec{v}) = -\nabla \mathrm{p} + \nabla \cdot \bar{\bar{\tau}} \,, \tag{2}$$

$$\frac{\partial}{\partial t}(\rho \mathrm{E}) + \nabla \cdot (\rho\overrightarrow{v_r}\mathrm{H} + \mathrm{p}\overrightarrow{u_r}) = \nabla \cdot (\kappa \nabla \mathrm{T} + \bar{\bar{\tau}} \cdot \vec{v}) \,, \tag{3}$$

where ρ stands for density , $\overrightarrow{v_r}$ is the relative velocity, p is the static pressure, $\overrightarrow{v_r}$ is the relative velocity, $\vec{\omega}$ is the angular velocity, E is the internal energy, H the total enthalpy and $\bar{\bar{\tau}}$ is the viscous stress. The source term $\vec{\omega} \times \vec{v}$ is the collapsed coriolis and centripetal accelerations for the absolute velocity formulation (ANSYS, 2018). The transformation from the inertial frame of reference to the rotating one is given by,

$$\nabla\vec{v} = \nabla\overrightarrow{v_r} + \nabla(\vec{\omega} \times \overrightarrow{r}) \,. \tag{4}$$

The equation that describes the circumferentially area averaging process for the mixing planes model is as follows,

$$\overline{f} = \frac{1}{A}\int_A f \, dA. \tag{5}$$

Here f stands for the variable that will be averaged, $\overline{f}$ is the averaged variable and A is area. Before solving them, the governing equations are time averaged and the extra terms produced because of this process due to the turbulent fluctuations are modelled using the k-w SST turbulence model (Menter, 1994). The time average Navier Stokes (RANS) equations solved here provides mean flow properties that are useful for engineering purposes (Versteeg & Malalasekera, 2005). Previous works (Goulos et al. 2018), (Mansour & Gunaraj, 2008), (Simões et al.,2009) have demonstrated the capabilities of the k-w SST turbulence model (Menter, 1994) for turbomachinery applications.

4. NUMERICAL MODELING

In this section, the numerical model used to carry out the aircraft turbofan engine simulations is described.

4.1 Flow solver

In this work, the numerical simulations are carried out using the commercial code Ansys Fluent (ANSYS, 2018). This tool uses a cell centered finite volume technique for solving the RANS transport equations. The steady state CFD simulations carried out were completed using a pressure based technique (ANSYS, 2018). The engine operating conditions simulated are shown in Tab. 1. This operating condition which closely correspond to typical top of climb (TOC) condition, has been selected due its importance in terms of fuel consumption and engine weight (Kerrebrock, 1992).

Table 1 Engine operating conditions

Parameter	Value
Mach number	0.85
Attitude	10 000 m.s.n.m
Absolute static pressure	23900 Pa
Temperature	218 K
Turbofan RPM	2261.5

4.2 Turbofan Engine geometry

The aircraft turbofan engine simulated in this work features an axisymmetric geometry resembling a GE90 turbofan engine. The nacelle and core geometries were obtained from a 3D analysis of a GE90 engine available in literature (Turner, 2000). The main engine geometry related data considered here is listed in Tab. 2 (Siddappaji, 2008). Figure 1 and Fig. 2 shows in turn details of geometric configurations simulated in this work.

Table 2 Geometry data of a GE90 like Turbofan engine

Parameter	
Overall Length	4775 mm
Intake/Fan diameter	3124 mm
Number of rotor blades	22
Number of stator blades (OGV)	24

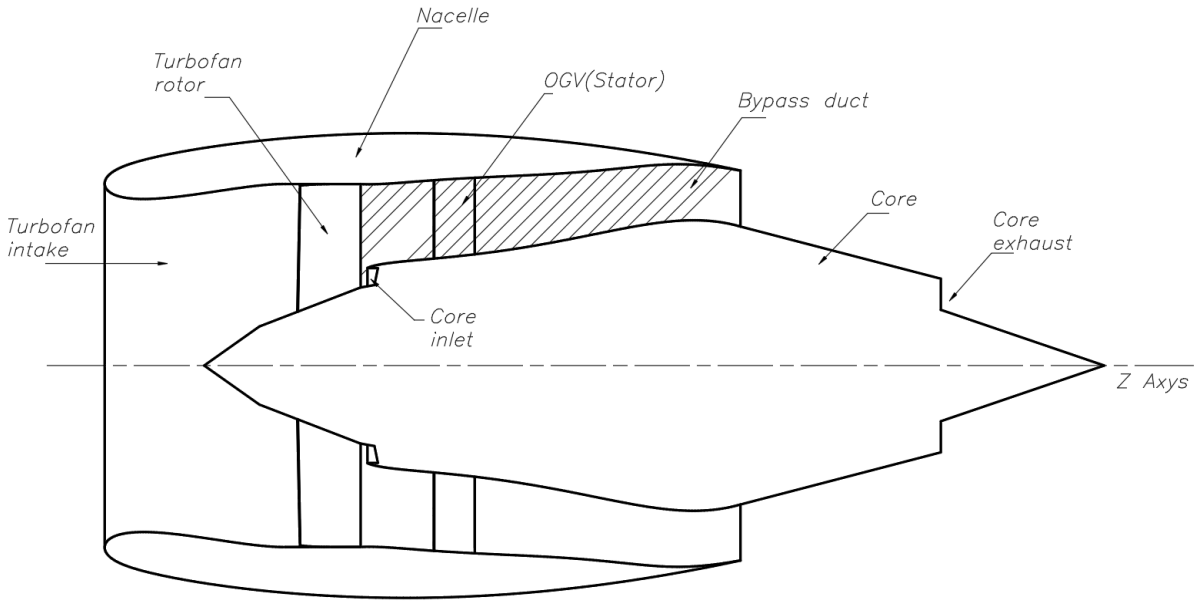

Figure 1. Turbofan engine geometry and main components.

4.2 Computational domain and boundary conditions

The computational domain simulated here features approximately 30D (engine diameters) in the axial direction and 20 D in the radial one as shown in Fig. 3. In this computational domain, far field boundary conditions are applied to the external boundaries , this kind of condition is based on the Riemann invariants to determine the flow variables at boundaries (ANSYS, 2018) . The required parameters for the external boundaries are the static pressure, velocity vectors and the turbulence viscosity ratio. A 5% of turbulent intensity and a turbulent viscosity ratio of 10 were imposed to all inlet and outlets. Two periodic boundary conditions were used, one of 16.36° for the rotor domain (22 blades) and the other of 15° for the stator domain (24 blades). Moreover, pressure outlet with radial equilibrium condition and mass flow rate inlet was set in the core inlet and outlet respectively. These parameters values come from flight conditions data and estimatives of the engine cycle. The corresponding numerical values accounted for are shown in Fig. 4. A solution hybrid initialization based on the far field quantities was carried out.

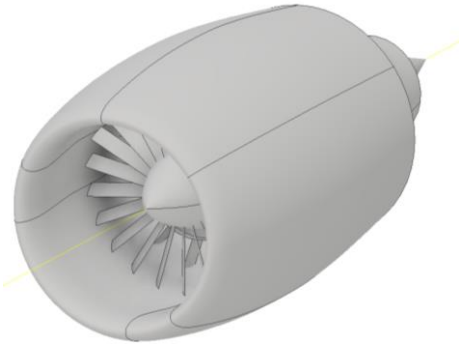

Figure 2 3D GE90 Turbofan Geometry

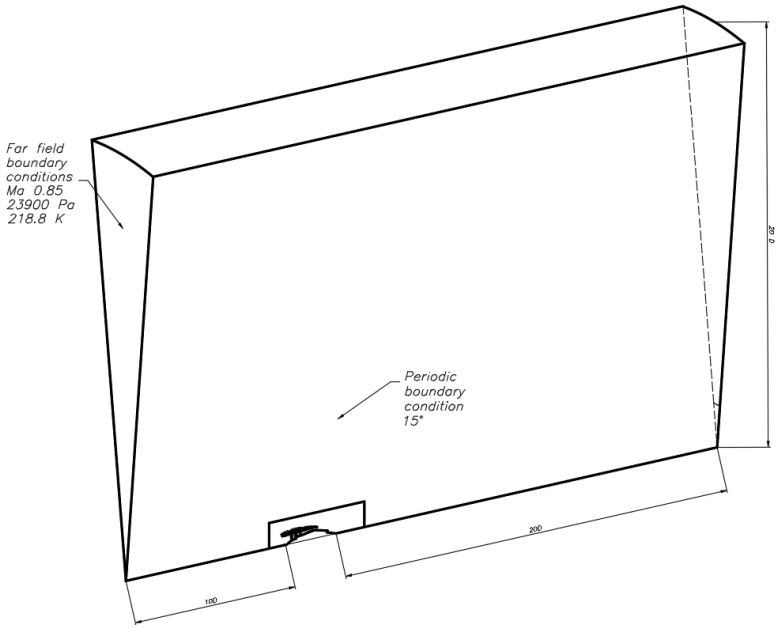

Figure 3 Extended computational domain

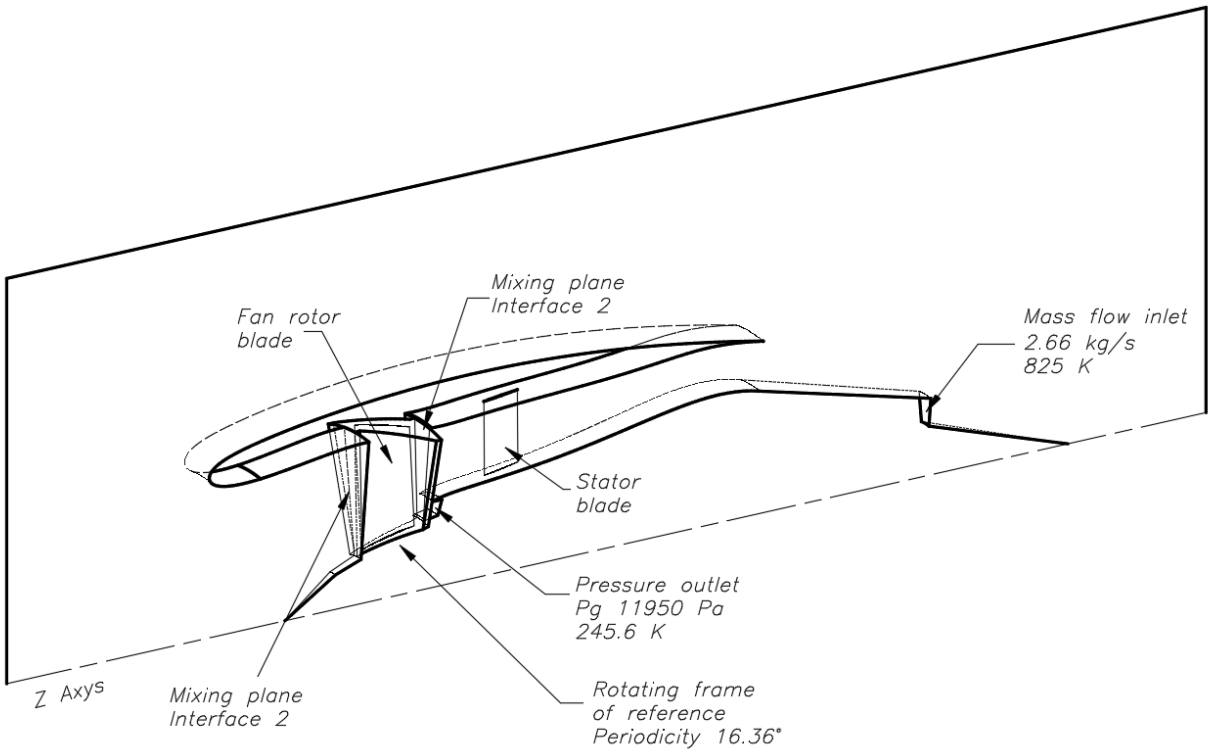

Figure 4. Computational domain and boundary conditions

4.3.2 Mesh generation

Ansys meshing (Ansys, 2018) was utilized to generate the computational meshes used in this work. Several grid sizes have been tried before defining the one utilized in this work. The computational domain was discretized using a multiblock unstructured grid due the relatively complex geometries involved . In addition, prism layers have been used near the walls to ensure a good boundary layer description. The bypass duct wall zones have been discretized using at least 30 prism cells with a grown rate of 1.2 as highlighted in Figure 5. A grid sensitive analysis has been performed to obtain grid independent results. Three grids featuring different levels of refinement have been assessed for this purpose. The body and face cell sizing at the bypass duct were decreased gradually between 50 and 25 mm. The number of nodes and elements characterizing the three grids evaluated here are show in Tab. 3. In Fig. 6 Mach number distribution along a

line in the axial direction is shown for the three mesh sizes studied. The mesh N°3 was used in this work obtaining the numerical results. The maximum relative error in Mach number between mesh N°2 and mesh N°3 was approximately 1 %.

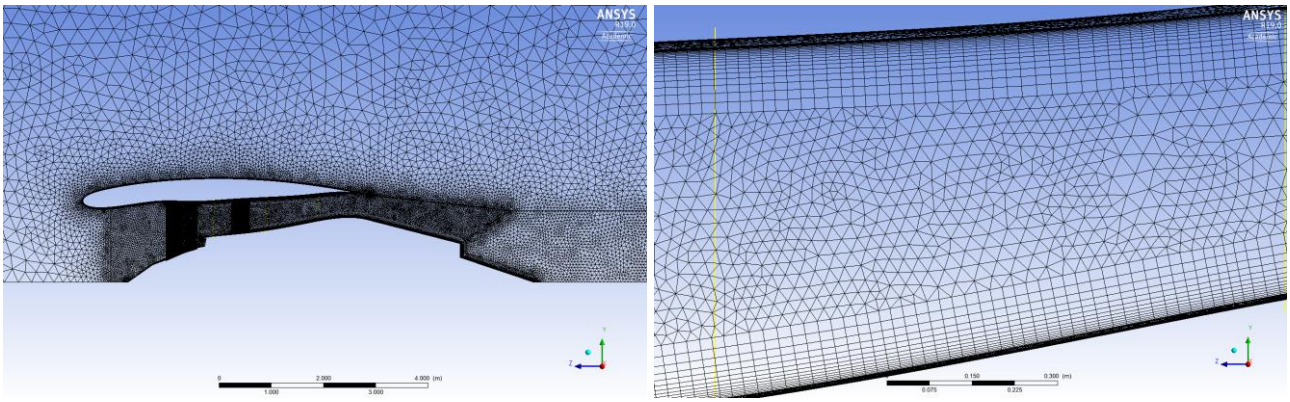

(a) (b)

Figure 5 Mesh details. (a) Turbofan engine unstructured mesh (b) Bypass duct unstructured mesh with prism layers to ensure good boundary layer description.

Table 3 Grid characteristics for grid dependence analysis

Mesh	Number of nodes	Number of elements
Mesh N°1	345422	1118963
Mesh N°2	616649	2218261
Mesh N°3	776294	2784197

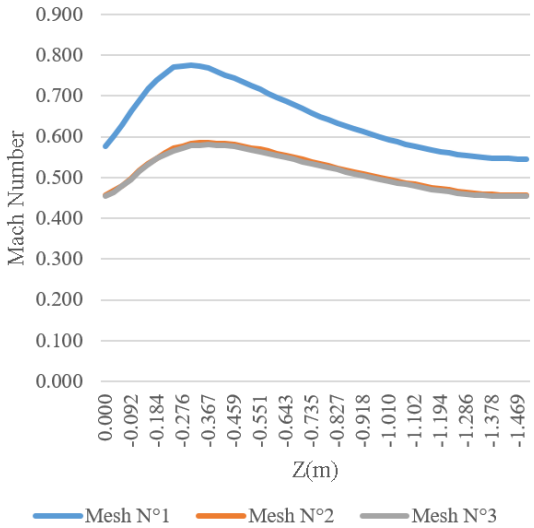

Figure 6 Mach number distribution for grid dependence analysis

5. RESULTS AND DISCUSSION

The main results obtained in this work can be divided into two sets of results. The first one presents representative contours at determined bypass duct engine locations. The referred locations are represented by stations in the z direction as shown in Figure 7. The second set of results presents plots in the span wise direction of representative quantities characterizing the flow structure.

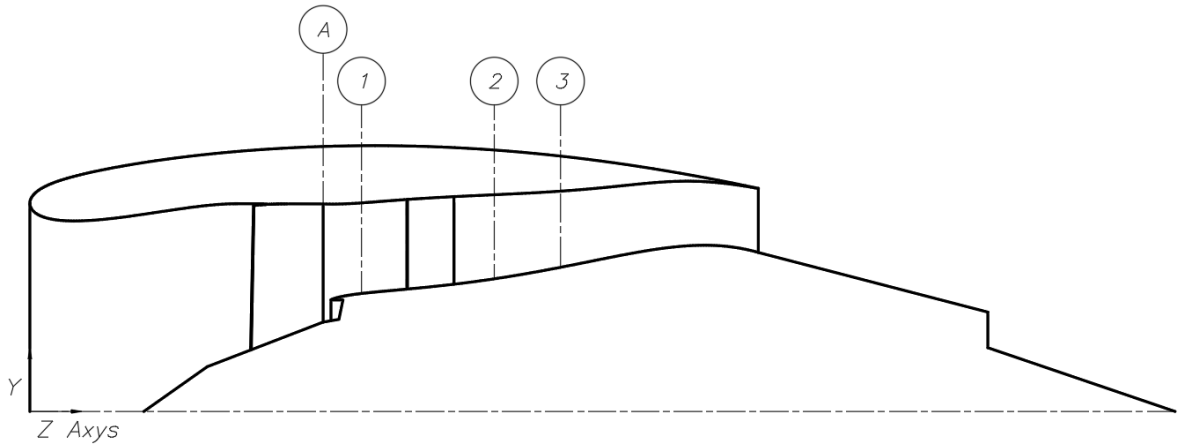

Figure 7. Particular engine stations accounted for in the analysis of results

The primary purpose of the exhaust system is to generate thrust through the acceleration of the airflow while minimizing pressure losses (Mattingly, 2006). The overall Mach number and static pressure distributions at the bypass duct and exhaust nozzle is presented in Fig. 8. It is interesting to note here that the flow behavior in the bypass duct is mainly transonic and becomes choked in the exit of the exhaust nozzle. In terms of flow pattern in the bypass duct and exhaust nozzle there is a good agreement between these results and those reported in the literature. According to Otter et al. (2018) and Goulos et al. (2018), during cruise conditions the bypass nozzle mostly operates under chocked conditions.

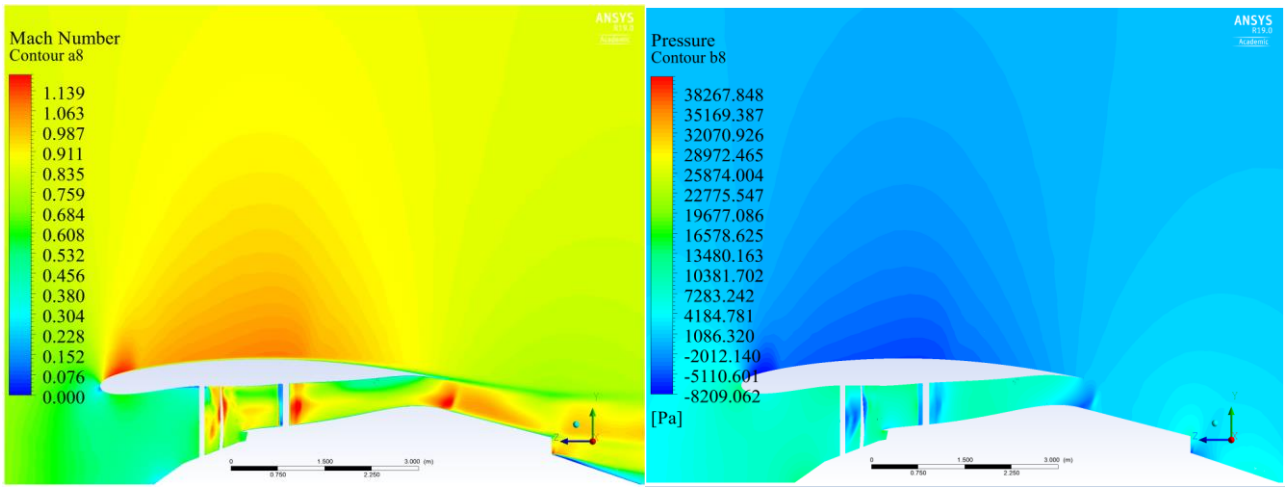

(a) (b)

Figure 8. Contours of (a) Mach number and (b)Static pressure at YX plane

In Figure 9 Mach number contours at the two faces of the mixing plane interface in Station 1 are presented. The results show that the outlet rotor domain has a distorted pattern Fig 9. (a). Moreover, the inlet profile Fig.9 (b) has a circumferentially uniform Mach number distribution . These results are consistent with the mixing planes approach theory. According to Denton (2016) this process introduce mixing losses that are assumed are the same as if the flow mixes with the downstream row. The analysis does not allow determining the distortion mechanisms in static pressure and temperature due to the radial flow unsteadiness, but provides a suitable boundary condition for the stator domain. As mentioned by Jerez et al. (2012) , the stagnation temperature, static pressure and flow distorted angles influence the shock structure over the OGV.

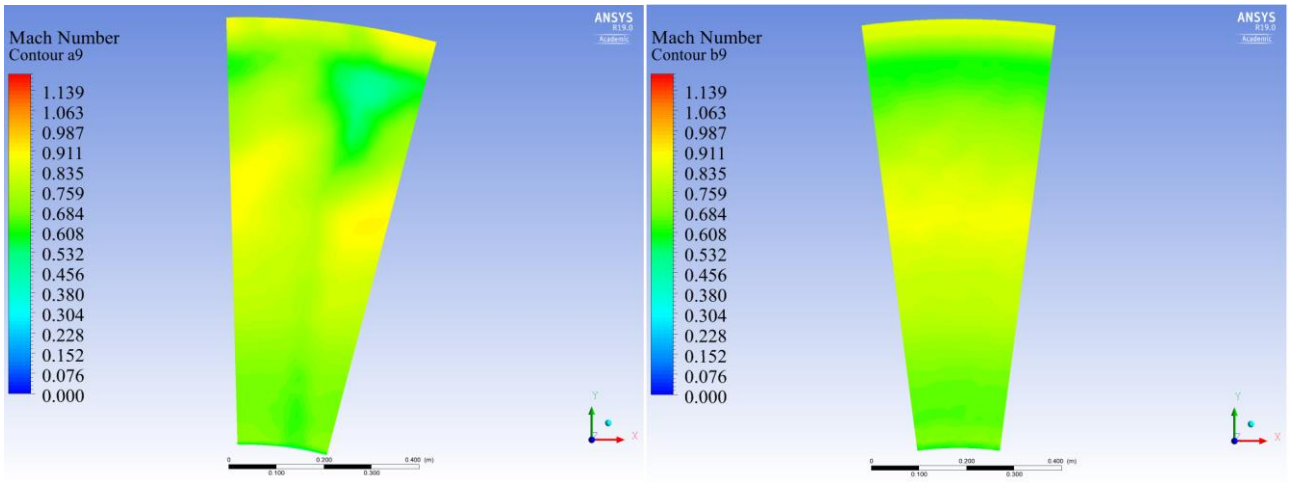

(b) (b)

Figure 9. Station A Mach number distributions (a) Outlet rotor (b) Inlet stator

As can be seen from Figure 10 and Figure 11 the flow pattern downstream the OGV (Stator) suggest that the flow becomes distorted. From Figure 10 (b) which shows the Mach number distribution after the OGV, it is observed in particular that, for the assessed geometry there is a flow separation in the stator blades. This separation affects of course the flow structure downstream the OGV. OGV geometry plays then an important role in the engine bypass duct flow pattern. The referred flow separation and the transonic flow change the flow patterns in the radial such changes become more pronunciated in the bypass duct upper section. Those results are compatible with Figure 12 (b) ones in term of flow separation in the upper section of the bypass duct.

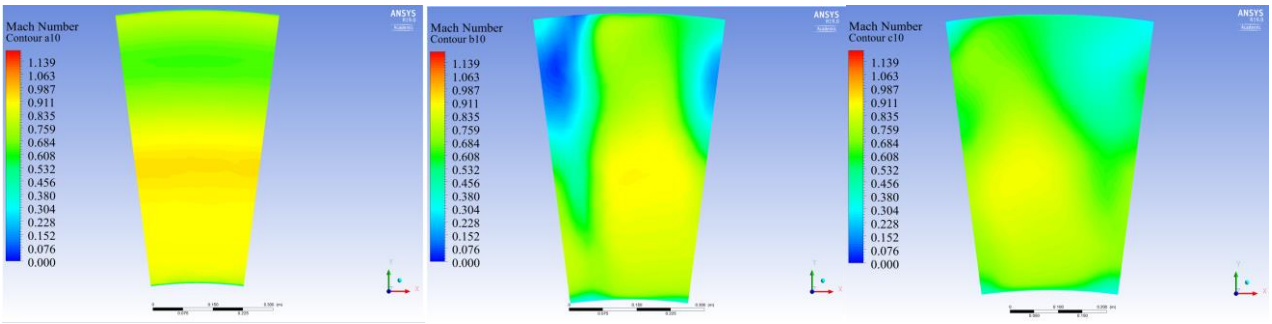

(a) (b) (c)

Figure 10 Mach number contours (a) Station 1 (b) Station 2 (c) Station3

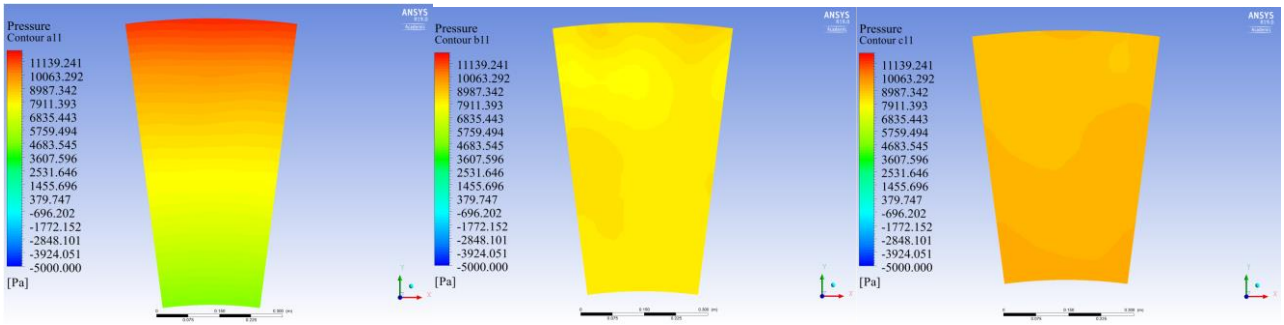

(a) (b) (c)

Figure 11 Static pressure contours (a) Station 1 (b) Station 2 (c) Station3.

Figure 12 shows static pressure and Mach number plots at the three station shown in Figure 7. The results highlight that the static pressure distribution becomes more uniform with the approach to the exhaust nozzle. This behavior in terms of static pressure is consistent with that observed by Odier et al. (2017).

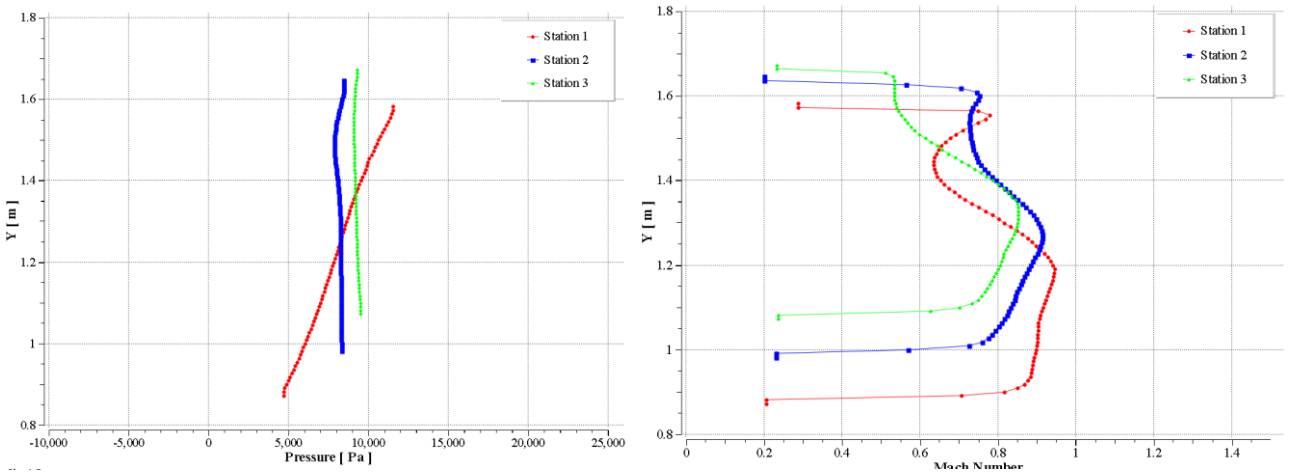

(a) (b)

Figure 12. (a) Static pressure and (b) Mach number distributions at a YZ plane along the Y direction.

From Fig. 11 (b) and Fig. 13 (b) it is noticed that the Mach number and the total pressure have similar distributions . These results are compatible with those obtained by Odier et al. (2017). The Fig. 13 (a) presents the total temperature distribution which increases in the radial direction and decreases in the axial direction approach to the exhaust nozzle . Again these results agree with previous findings (Odier et al., 2017)

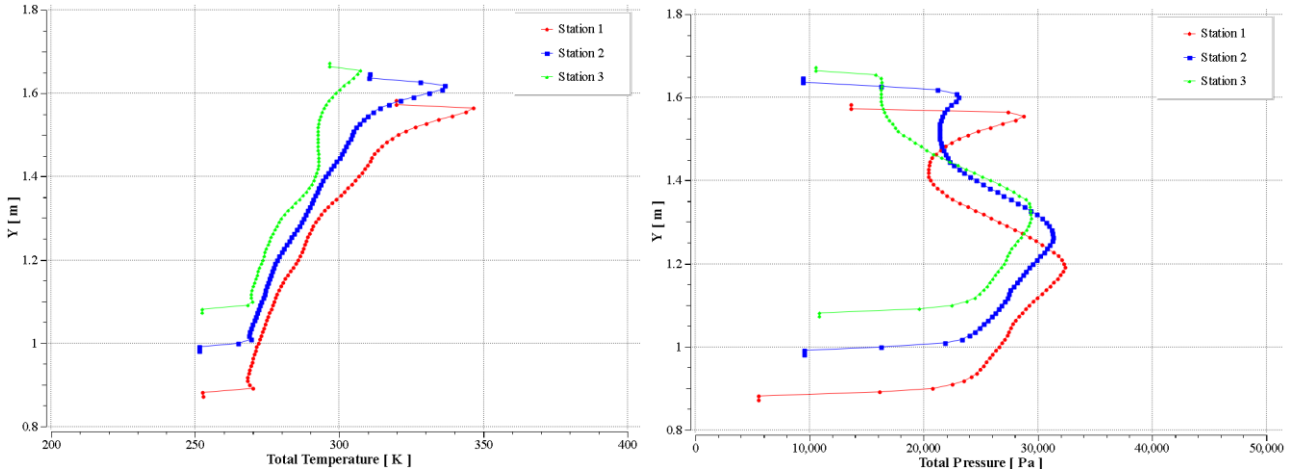

(a) (b)

Figure 13. (a) Total temperature and (b) Total pressure distributions at a YZ plane along the Y direction.

6. CONCLUSSIONS

The aerodynamics of GE90 like turbofan bypass duct has been investigated by means of a mixing planes steady state approach accounting for the rotor effects in the flow structure. Previous works in the field of exhaust system and turbo machinery modeling were used to verify the computed flow structure, demonstrating the suitability of this method for these particular applications. Based on the results, it can be concluded that the bypass flow structure under cruise conditions is mostly transonic and presents a choked condition in the exhaust nozzle. The Mach number, static pressure, total temperature and total pressure distribution are in relative good agreement with previous findings. The results obtained here indicate that the stator geometry significantly influences the bypass duct flow structure, ´playing thus an important role in the design of exhaust systems. The findings from this works suggest that the mixing planes approach could be useful for studying new bypass duct concepts. Future work will involve modifying the bypass duct flow structure though the use of devices focusing the improvement of turbofan engine performance.

7. REFERENCES

Abdol-Hamid, K. S., Uenishi, K., Keith, B. D., & Carlson, J. R. (1993). Commercial turbofan engine exhaust nozzle flow analyses. *Journal of Propulsion …*, *9*(3), 431–436. https://doi.org/10.2514/3.23639

Adamczyk, J. J. (2000). Aerodynamic Analysis of Multistage Turbomachinery Flows in Support of Aerodynamic Design. *Journal of Turbomachinery*, *122*(2), 189. https://doi.org/10.1115/1.555439

Ansys. (2018). ANSYS Meshing User's Guide.

ANSYS. (2018). ANSYS Fluent Theory Guide, (January).

Biesinger, T., Cornelius, C., Rube, C., Braune, A., Campregher, R., Godin, P. G., … Zori, L. (2010). Unsteady CFD Methods in a Commercial Solver for Turbomachinery Applications. *ASME Conference Proceedings*, *2010*(44021), 2441–2452. https://doi.org/10.1115/GT2010-22762

Boeing. (2012). Boeing Long Term Market: Current Market Outlook 2015–2034. *Boeing Technical Report*.

Calvert, W. J., & Cinder, R. B. (1999). Transonic fan and compressor design. *Proceedings of the Institution of Mechanical Engineers, Part C: Journal of Mechanical Engineering*, *213*(5), 419–436. https://doi.org/10.1243/0954406991522671

Cumpsty, N. A. (2010). Preparing for the Future: Reducing Gas Turbine Environmental Impact—IGTI Scholar Lecture. *Journal of Turbomachinery*, *132*(4), 041017. https://doi.org/10.1115/1.4001221

Denton, J. D. (1992). The Calculation of Three-Dimensional Viscous Flow Through Multistage Turbomachines. *Journal of Turbomachinery*, *114*(1), 18. https://doi.org/10.1115/1.2927983

Denton, J. D. (2016). Some Limitations of turbomachinery CFD. In *oceedings of the ASME Turbo Expo 2010* (pp. 1–11).

Dixon, S. L., Dixon, S. L., & Hall, C. A. (2013). *Fluid Mechanics and Thermodynamics of Turbomachinery*. Butterworth-Heinemann/Elsevier. Retrieved from https://books.google.com.pe/books?id=CEpipwAACAAJ

Fluent. (2011). ANSYS FLUENT User ' s Guide, *15317*(November), 2498. Retrieved from http://cdlab2.fluid.tuwien.ac.at/LEHRE/TURB/Fluent.Inc/v140/flu_ug.pdf

Godard, B., Jaeghere, E. De, Ben, N., Marty, J., Barrier, R., & Gourdain, N. (2017). "A review of Inlet Fan Coupling Methodologies." *Proceeding of ASME Turbo Expo 2017, GT 2017-63*.

Goulos, I., Stankowski, T., MacManus, D., Woodrow, P., & Sheaf, C. (2018). Civil turbofan engine exhaust aerodynamics: Impact of bypass nozzle after-body design. *Aerospace Science and Technology*, *73*, 85–95. https://doi.org/10.1016/j.ast.2017.09.002

Greitzer, E. M., Tan, C. S., & Graf, M. B. (2004). *Internal Flow: Concepts and Applications*. *Cambridge Engine Technology Series*. https://doi.org/DOI: 10.1017/CBO9780511616709

IATA. (2015). IATA Air Passenger Forecast Shows Dip in Long-Term Demand. *IATA Pressroom*, *55*(November), 7–12. Retrieved from http://www.iata.org/pressroom/pr/Pages/2015-11-26-01.aspx

International Civil Aviation Organization. (2013). "Present and Future Trends in Aircraft Noise and Emissions. TR A39-WP/55 EX/32.

Jerez Fidalgo, V., Hall, C., & Collin, Y. (2012). "A study of Fan-Distortion Interaction Whitin the NASA Rotor 67 Transonic Stage." *Journal of Turbomachinery*, *134*, ASME.

Kellari, D., Crawley, E. F., & Cameron, B. G. (2017). Influence of Technology Trends on Future Aircraft Architecture. *Journal of Aircraft*, 1–15. https://doi.org/10.2514/1.C034266

Kerrebrock, J. (1992). Aircraft Engines and Gas Turbines. *Aircraft Engines and Gas Turbines (2nd Edition)*, 26–29. https://doi.org/10.1080/03043799208923198

Kim, S., Yang, S., Lee, D., Baftalovski, S., & Makarov, V. (1999). Three-dimensional flow calculation around/through isolated nacelle with an actuator disk modeling. In *35th Joint Propulsion Conference and Exhibit*. American Institute of Aeronautics and Astronautics. https://doi.org/doi:10.2514/6.1999-2668

Lee, J. J., Lukachko, S. P., Waitz, I. A., & Schafer, A. (2001). Historical and Future Trends in Aircraft Performance, Cost and Emissions. *Annual Review of Energy and the Environment*, *26*(1), 167–200. https://doi.org/10.1146/annurev.energy.26.1.167

MacIsaac, B., & Langton, R. (2011). *Gas Turbine Propulsion Systems*. *Gas Turbine Propulsion Systems*. https://doi.org/10.1002/9781119975489

Mansour, M. L., & Gunaraj, J. (2008). Validation of Steady Average-Passage and Mixing Plane CFD Approaches for the Performance Prediction of a Modern Gas Turbine Multistage Axial Compressor. *ASME Turbo Expo 2008: Power for Land, Sea, and Air (GT2008)*, 1–11. https://doi.org/10.1115/GT2008-50653

Marble, F. (1964). "Three-Dimensional Flow in Turbomachines",. *High Speed Aerodynamics and Jet Propulsion*, *X*, Hawthorne, ed, Princeton University Press.

Mattingly, J. D. (2006). *Elements of propulsion:Gas turbines and Rockets*. *AIAA Educational series*. https://doi.org/10.2514/4.861789

Maunus, J., Grace, S., Sondak, D., & Yakhot, V. (2012). Characteristics of Turbulence in a Turbofan Stage. *Journal of Turbomachinery*, *135*(2), 21010–21024. Retrieved from http://dx.doi.org/10.1115/1.4006774

Menter, F. R. (1994). Two-equation eddy-viscosity turbulence models for engineering applications. *AIAA Journal*, *32*(8), 1598–1605. https://doi.org/10.2514/3.12149

Montomoli, F., Carnevale, M., D'Ammaro, A., Massini, M., & Salvadori, S. (2015). Uncertainty Quantification in Computational Fluid Dynamics and Aircraft Engines, 21–33. https://doi.org/10.1007/978-3-319-14681-2

Odier, N., Duchaine, F., & Gicquel, L. . (2017). Comparison of LES and RANS predictions with experimental results of the fan of a turbofan. In *European Conference on Turbomachinery Fluid dynamics & Thermodynamics*. Stockholm,Sweden.

Otter, J. J., Goulos, I., MacManus, D. G., & Slaby, M. (2018). Aerodynamic Analysis of Civil Aeroengine Exhaust Systems Using Computational Fluid Dynamics. *Journal of Propulsion and Power*, 1–14. https://doi.org/10.2514/1.B36867

Peters, A. (2014). "Ultra-short nacelles for low fan pressure ratio propulsors," (PhD t).

Pontes, M. C. (2015). *US 9,222,436 B2*. United States.

Schnell, R., Schönweitz, D., Theune, M., & Corroyer, J. (2016). Integration- and Intake-Induced Flow Distortions and Their Impact on Aerodynamic Fan Performance BT - Advances in Simulation of Wing and Nacelle Stall. In R. Radespiel, R. Niehuis, N. Kroll, & K. Behrends (Eds.) (pp. 251–269). Cham: Springer International Publishing.

Siddappaji, K. (2008). *Benefits of GE90 representative turbofan through cycle analysis*.

Simões, M. R., Montojos, B. G., Moura, N. R., & Su, J. (2009). VALIDATION OF TURBULENCE MODELS FOR SIMULATION OF AXIAL FLOW COMPRESSOR. *COBEM*, 1–9. Retrieved from http://www.fem.unicamp.br/~phoenics/EM974/PROJETOS/Temas Projetos/Axial Compressor/COB09-3328.pdf

Trancossi, M., & Madonia, M. (2012). The Efficiency of an Electric Turbofan vs. Inlet Area: A Simple Mathematical Model and CFD Simulations. In *SAE Technical Paper*. SAE International. https://doi.org/10.4271/2012-01-2217

Turner, M. (2000). *Full 3D Analysis of the GE90 Turbofan Primary Flowpath*. Cincinnati,Ohio.

Versteeg, H. K., & Malalasekera, W. (2005). *Introduction to Computational Fluid Dynamics*. *Science* (Vol. 44). https://doi.org/10.2514/1.22547

8. RESPONSIBILITY NOTICE

The authors are the only responsible for the printed material included in this paper.